

Plasma Sci. Technol. **20** (2018) 014002 (8pp) https://doi.org/10.1088/2058-6272/aa9326

NO reduction using low-temperature SCR assisted by a DBD method

Yanghaichao LIU (刘杨海超)[1], Renxi ZHANG (张仁熙)[1], Huiqi HOU (侯惠奇)[1], Shanping CHEN (陈善平)[2] and Ruina ZHANG (张瑞娜)[2]

[1] Shanghai Key Laboratory of Atmospheric Particle Pollution and Prevention (LAP[3]), Institute of Environmental Science, Fudan University, Shanghai 200433, People's Republic of China
[2] Shanghai Institute for Design & Research on Environmental Engineering, Shanghai 200232, People's Republic of China

E-mail: zrx@fudan.edu.cn

Received 29 July 2017, revised 9 October 2017
Accepted for publication 11 October 2017
Published 28 November 2017

Abstract

This paper discusses the removal of nitric oxide (NO) with low-temperature selective catalytic reduction driven by a dielectric barrier discharge with ammonia (NH_3) as a reductant. We explored the effects of NH_3, O_2, temperature and water under different applied voltage on NO removal at atmospheric pressure. The results showed that when the gas concentration ration of NH_3/NO was 0.23–0.67, the NO removal efficiency and the energy consumption was acceptable. The NO removal efficiency reached 84% under an applied voltage of 7 kV, 400 ppm NO and 90 ppm NH_3 at a temperature of 150 °C. Water vapor had a negative effect because NO formation reactions were strengthened and NH_3 was oxidized directly rather than reduced NO molecules. The outlet gas components were observed via Fourier transform infrared spectroscopy for revealing the decomposition process and mechanism.

Keywords: dielectric barrier discharge, NO, NH_3, SCR

(Some figures may appear in colour only in the online journal)

1. Introduction

Nitric oxide (NO_x), as one of the major factors responsible for serious problems such as acid rain, photochemical smog and $PM_{2.5}$, does great damage to the environment and human health [1, 2]. The removal of nitric oxide has become one of the most challenging issues for the coming decade. The selective catalytic reduction (SCR) method, which generally uses NH_3 as a reductant and V_2O_5–WO_3/TiO_2 as a cost-effective catalyst, has been wildly applied to NO removal in industrial application projects since the 1990s [3–5]. However, the typical V_2O_5–WO_3/TiO_2 catalyst shows high performance only within the narrow temperature window of 300–450 °C [6–8]. In actual NO removal application, the NH_3–SCR system is usually set upstream of dust precipitation and the desulfurization system, avoiding reheating the flue gas, but easily resulting in catalyst abrasion or poisoning and damage by sulfur-containing gas. Thus, an effective low-temperature NH_3–SCR system is a new focus in the current study [9, 10].

To improve the low-temperature NH_3–SCR system performance, many new kinds of precious metal catalysts have been developed [11–13]. Although these new catalysts have shown acceptable results under lower temperature, they could be easily damaged or deactivated by other gas components such as sulfur dioxide, water and dust [14–17]. In addition to the harsh requirements of reactant gas composition, these metal catalysts are also very expensive and not applicable currently in practical applications.

Some literature studies have shown that the plasma technique has relatively high catalytic activation under low-temperature [18–23]. Dielectric barrier discharge (DBD) can generate a non-thermal plasma at atmosphere pressure with the advantage of compact systems and fast or easy reactivity under low-temperature [24]. Recently, a combination of the NH_3–SCR method and the DBD technique has been of interest for application in low-temperature SCR processes [6, 25, 26], for example, Guan *et al* found that the combination of NH_3–SCR and a non-thermal plasma enhanced the overall reaction and allowed for an effective removal of NO_x

at 100 °C [6], and Wang *et al* studied NO removal in a plasma–catalyst system over CuCe/ZSM-5 catalysts and observed the highest NO and NO_x removal efficiencies of 90.7% and 80.1% [26]. However, there are few reports concerning the denitration reaction mechanism and the effect of extra oxidation of NH_3 induced by the active particles in the DBD plasma system, and the optimum operation conditions for NO_x removal is also needed to be cleared using the NH_3–SCR system assisted by DBD [27, 28]. As the most widely used catalyst in practical business applications, the typical V_2O_5–WO_3/TiO_2 catalyst shows high performance only within the narrow temperature window of 300–450 °C [6]. However, in the combined NH_3–SCR and DBD system, the catalytic activity performance of the V_2O_5–WO_3/TiO_2 catalyst at lower temperatures is needed, especially under the conditions of high gas hourly space velocity (GHSV).

In this paper, a study was performed of a NH_3–SCR system assisted by an *in situ* DBD reactor. In the new integrated NH_3–SCR DBD reactor, V_2O_5–WO_3/TiO_2 was placed in the discharge area for achieving high catalytic activation under low temperature (25–150 °C). The effects of NH_3, oxygen, temperature and H_2O under varied applied voltage on NO_x removal were explored. We also analyzed the reaction products to reveal the mechanism of NO_x abatement. The results could provide useful information and suggestions on treating NO for industrial applications.

2. Experiment section

A schematic diagram of the NH_3–SCR–DBD system is presented in figure 1. The inlet gases consisting of NO, N_2, NH_3 and O_2, are controlled by a mass flow controller (Horiba Stec-4400, JPN) and mixed with a gas blender. The mixed gases pass through a buffer chamber and then are led into the DBD reactor. The reactor consisted of an inner high-voltage electrode (graphite), two quartz tubes (outer tube with 30 mm inner diameter and 200 mm length, inner tube with 6 mm outer diameter and 300 mm length), and an outer electrode (aluminum foil). The quartz tubes were coaxial cylinder in shape with a 12 mm gap. The catalysts of V_2O_5–WO_3/TiO_2 (Hunan Xinrui Co., CN) were packed evenly in the discharge area.

2.1. Measurements of electrical properties

The DBD power supply can provide a sinusoidal alternating voltage varying from 5 kV to 20 kV at frequency of 10–20 kHz. The voltage and power applied was measured via the voltage-charge Lissajous figure with a 200 MHz digital phosphor oscilloscope (Tektronix, TDS2024B, USA) connected to a 1000:1 HV probe (Tektronix P6015A, USA). The current was obtained by measuring the voltage of a resistor, and the Lissajous figure was measured at the discharge electrode and 0.47 μF equivalent capacitor. Figure 2(a) shows the voltage waveforms at the discharge electrode and figure 2(b) shows the corresponding charge–voltage Lissajous figure. As shown in figure 2, the cycle A-B-C-D-A corresponds to the variation of a discharge cycle.

2.2. Measurements of gas content

All the gaseous components concentrations were continuously quantified using a Fourier transform infrared absorption spectrometer (FTIR, FTIR 850, Tianjin Gangdong Co., CN). Removal efficiency (η_{NO}), specific energy density (*SED*), and energy consumption (E_{NO}) were defined as follows:

$$\eta_{NO} = \frac{(NO_{in} - NO_{out})}{NO_{in}} \times 100\%$$

$$SED = \frac{P}{Q}$$

$$E_{NO} = \frac{10\,000P}{36Q(NO_{in} - NO_{out})}$$

where NO_{in} and NO_{out} are the inlet and outlet concentrations of NO (ppm), respectively; Q is the gas flow rate (l s^{-1}); P is the input power (W); *SED* is the specific energy density (J l^{-1}); and E_{NO} is energy consumption (kWh kg^{-1}).

3. Results and discussion

3.1. Ammonia (NH_3) effects

Figure 3(a) showed the effect of NH_3 upon removal efficiency of NO and energy consumption in a packed bed DBD reactor with an initial NO concentration of 400 ppm, and an inlet NH_3 concentration of 90 ppm. The applied voltage was adjusted from 2 kV to 7 kV. The GHSV was 19 420 h^{-1}. The experimental temperature was 25 ± 3 °C except for the additional requirement on the temperature.

The results indicate that the addition of NH_3 significantly contributed to the removal efficiency of NO. With the increase in applied voltage of 4 kV to 7 kV, the NO removal efficiency was improved from 70% to 87% in the presence of NH_3. The E_{NO} (energy consumption of NO) decreased with the increasing voltage, and at the same applied voltage, NH_3 have a positive effect on E_{NO}.

When the applied voltage increased, the electric field of the system increased both in the absence and in the presence of NH_3, and the numbers of high-energy electrons and particles were also improved as a result of higher probability of collision between NO molecules and electrons or particles. The energy consumption decreased in the presence of NH_3 because more NO molecules were removed under the same applied voltage. With the production of lots of new high-energy particles such as NH_2·, NH·, H·, the collision reactions of NO molecules were greatly enhanced.

When the concentration of NH_3 varied from 0 ppm to 450 ppm, the effect of NH_3 concentration on NO removal efficiency and energy consumption are shown in figure 2(b) under the initial NO concentration of 400 ppm and the applied voltage of 4 kV.

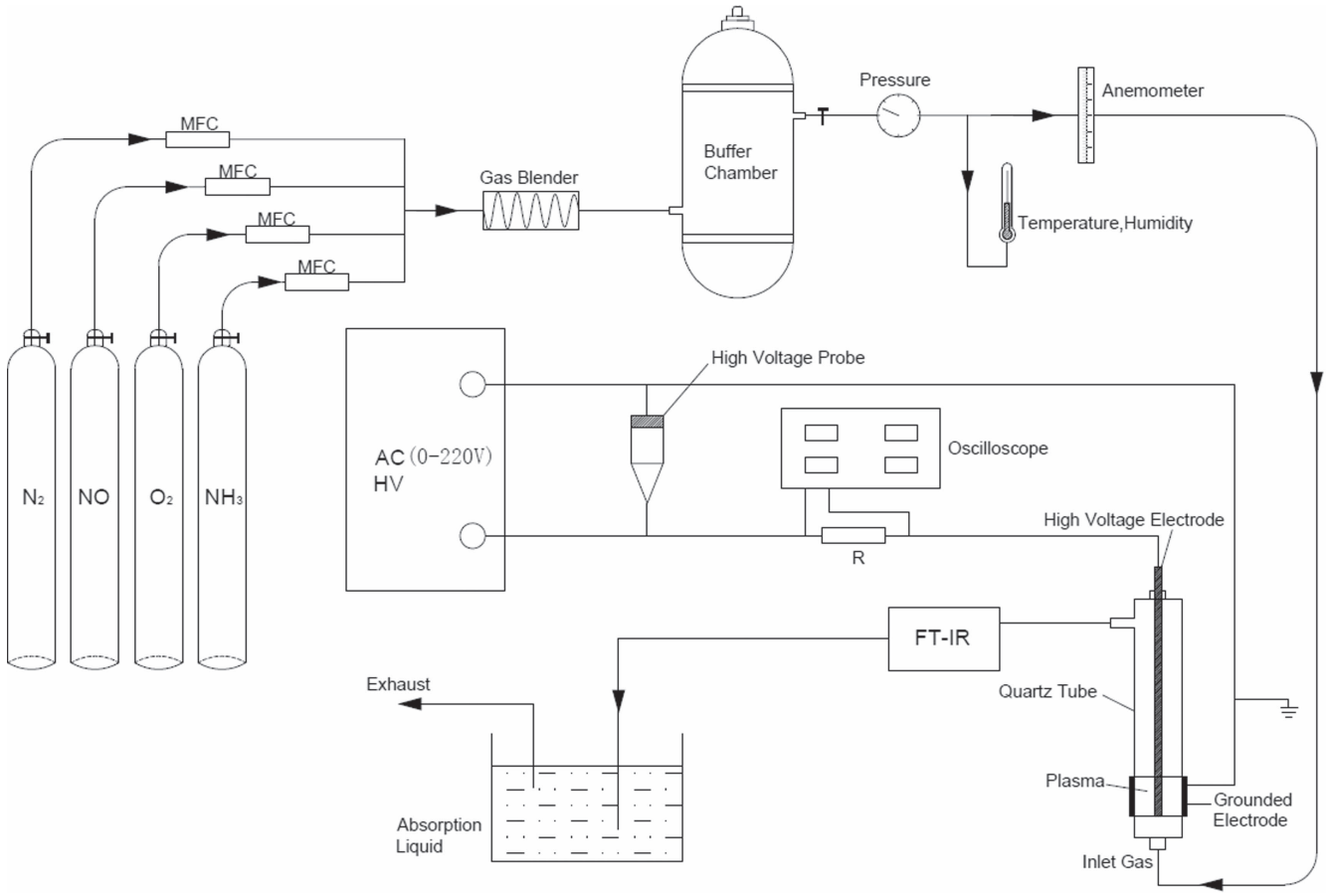

Figure 1. Schematic diagram of the experimental setup of the NH_3–SCR–DBD system.

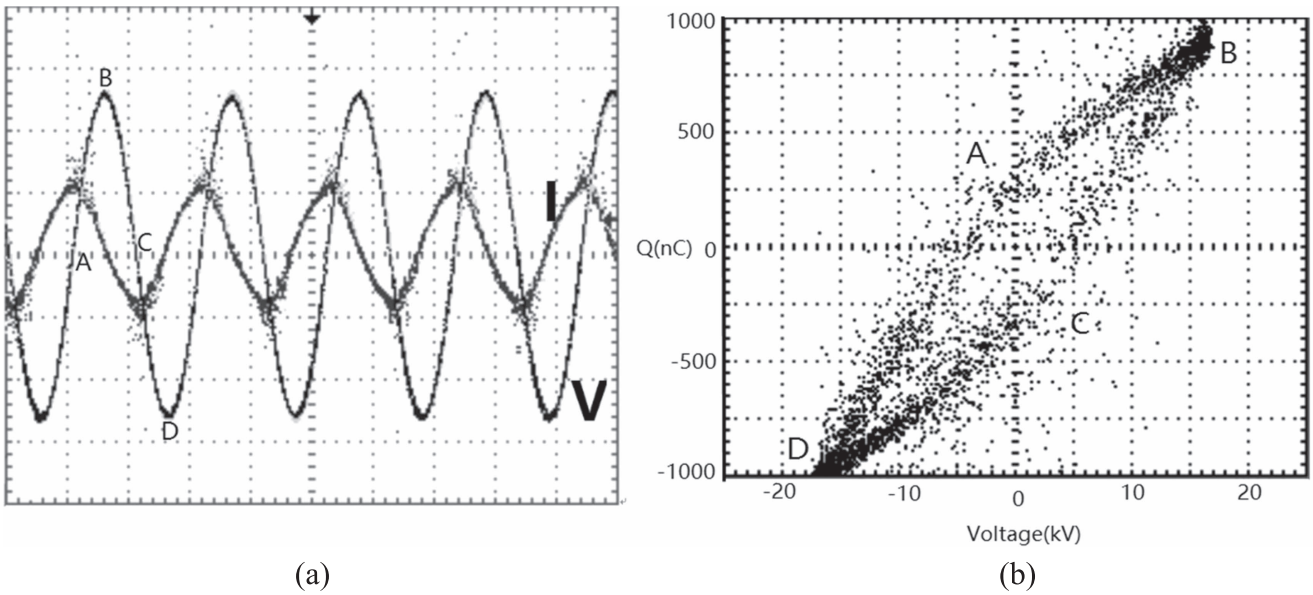

Figure 2. (a) Voltage waveforms measured at the discharge electrode. (b) Corresponding charge–voltage Lissajous figure.

Figure 3(b) shows that with the increase in initial NH_3 concentration, the removal efficiency of NO increased but energy consumption decreased. However, when the NH_3 concentration was more than 270 ppm, the NO removal efficiency decreased while E_{NO} increased slightly. η_{NO} decreased to 67% and E_{NO} was 16.49 kWh kg^{-1} when the content of NH_3 was 450 ppm. When the NH_3 concentration was 270 ppm, η_{NO} reached a maximum of 72% and the E_{NO} was 15.62 kWh kg^{-1}.

With more NH_3 molecules induced into the reaction system, the total quantity of collision particles increased, and more active free radicals such as NH_2·, NH·, H· were also

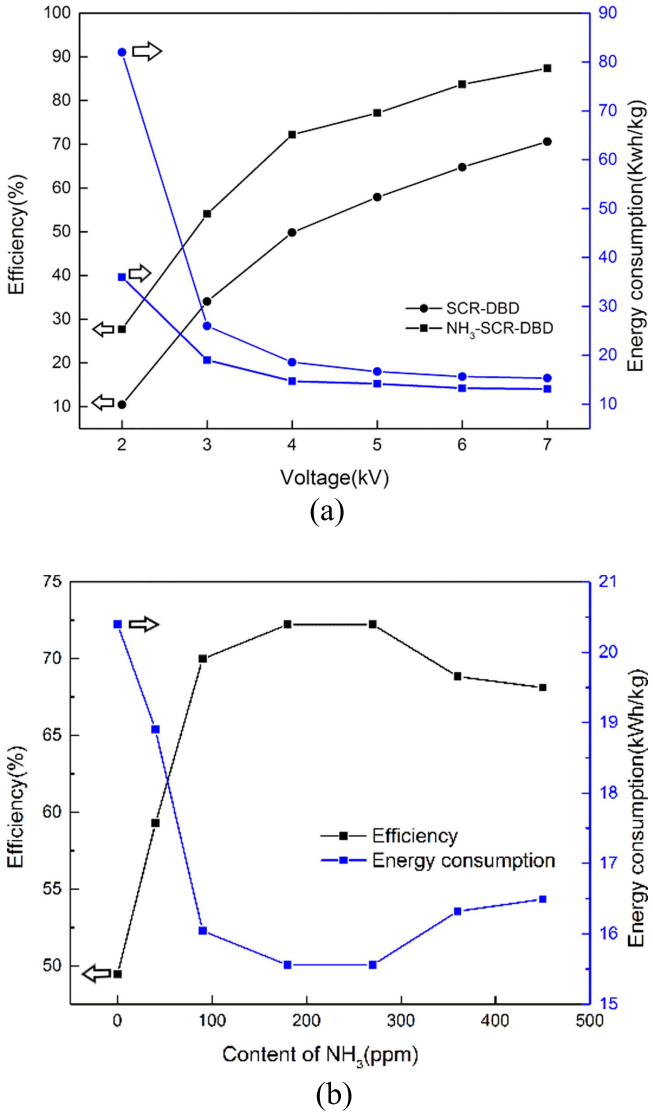

Figure 3. (a) The effect of NH_3 on the removal efficiency of NO and energy consumption. (b) The effect of different NH_3 concentration.

involved in the reaction process, which could significantly contribute to the removal of NO molecules (reactions R3, R4 and R5). However, when the NH_3 concentration was more than 270 ppm, superfluous ammonia molecules could be oxidized by oxygen, which could lead to NO formation (reactions R6 and R7).

$$\cdot OH + NH_3 \rightarrow H_2O + \cdot NH_2 \quad k(25\ ^\circ C) = 1.6 \times 10^{-13}\ [29] \tag{R1}$$

$$\cdot OH + \cdot NH_2 \rightarrow H_2O + \cdot NH \quad k(25\ ^\circ C) = 1.7 \times 10^{-12}\ [30] \tag{R2}$$

$$NO + \cdot NH_2 \rightarrow N_2 + H_2O \quad k(25\ ^\circ C) = 1.2 \times 10^{-11}\ [31] \tag{R3}$$

$$\cdot NH + NO \rightarrow N_2O + \cdot H \quad k(25\ ^\circ C) = 2.9 \times 10^{-11}\ [32] \tag{R4}$$

$$\cdot NH + NO \rightarrow \cdot OH + N_2 \quad k(25\ ^\circ C) = 4.8 \times 10^{-12}\ [32] \tag{R5}$$

$$\cdot NH + \cdot O \rightarrow \cdot H + NO \quad k(25\ ^\circ C) = 1.2 \times 10^{-10}\ [30] \tag{R6}$$

$$\cdot NH + O_2 \rightarrow \cdot OH + NO \quad k(25\ ^\circ C) = 9.0 \times 10^{-15}\ [33]. \tag{R7}$$

Consequently, the removal efficiency of NO could decrease slightly and E_{NO} increased when too many NH_3 molecules were led into the reactor. We could achieve an attractive removal efficiency with low energy consumption under atmospheric pressure and low-temperature conditions when the concentration of NH_3 varied from 90 ppm to 270 ppm. The gas concentration ratio of NH_3/NO at 0.23–0.67 proved to be very attractive.

3.2. Oxygen (O_2) effects

Figure 4(a) shows the relationship between applied voltage and removal efficiency of NO under different percentages of oxygen (0%, 2% and 8%) conditions. The initial concentration of NO and NH_3 were 400 ppm and 90 ppm, respectively. The applied voltage varied from 2 kV to 7 kV. Figure 3(b) shows NO and NO_2 concentration under the same conditions.

The data shown in figure 4(a) indicate that the removal efficiency of NO increased gradually with the increase in applied voltage, and decreased with the oxygen concentration under the same applied voltage. In the presence of oxygen, the DBD process produces ozone and degrades NO

$$O_2 + O \rightarrow O_3 \tag{R8}$$

$$O_3 + NO \rightarrow NO_2 + O_2. \tag{R9}$$

However, from the results, the NO removal process was suppressed because NO and NH_3 were partially oxidized to new NO and NO_2. Therefore, the removal efficiency of NO decreased. The main reactions occurred in the presence of O_2 and O_3 and are listed as follows:

$$\cdot NH + \cdot O \rightarrow \cdot H + NO \tag{R10}$$

$$\cdot NH + O_2 \rightarrow \cdot OH + NO \tag{R11}$$

$$2NH_3 + 2O_2 \rightarrow N_2O + 3H_2O \tag{R12}$$

$$2NH_3 + \frac{5}{2}O_2 \rightarrow 2NO + 3H_2O \tag{R13}$$

$$2NH_3 + \frac{5}{3}O_3 \rightarrow 2NO + 3H_2O. \tag{R14}$$

Therefore, when more oxygen molecules were induced into the reaction system, lots of active radicals such as ·O were generated. Then, large quantities of NH_3 were oxidized to NO molecules, which acted as a negative effect on NO removal.

As shown in figure 4(b), the concentration of NO decreased quickly and NO_2 increased slightly in the presence of O_2 molecules when the applied voltage was below 3 kV. Then, with the applied voltage continually increasing, the NO and NO_2 concentrations decreased slightly. Initially, under the low O_2 concentration, lots of NO molecules were degraded (as shown in R3 to R5). However, higher O_2 concentration led to NO_2 molecule formation, and, at the same time, with higher applied voltage, the electric field of the reaction system was strengthened, and more NH_3 molecules participated in the reactions with O_2 and ·O, which led to new

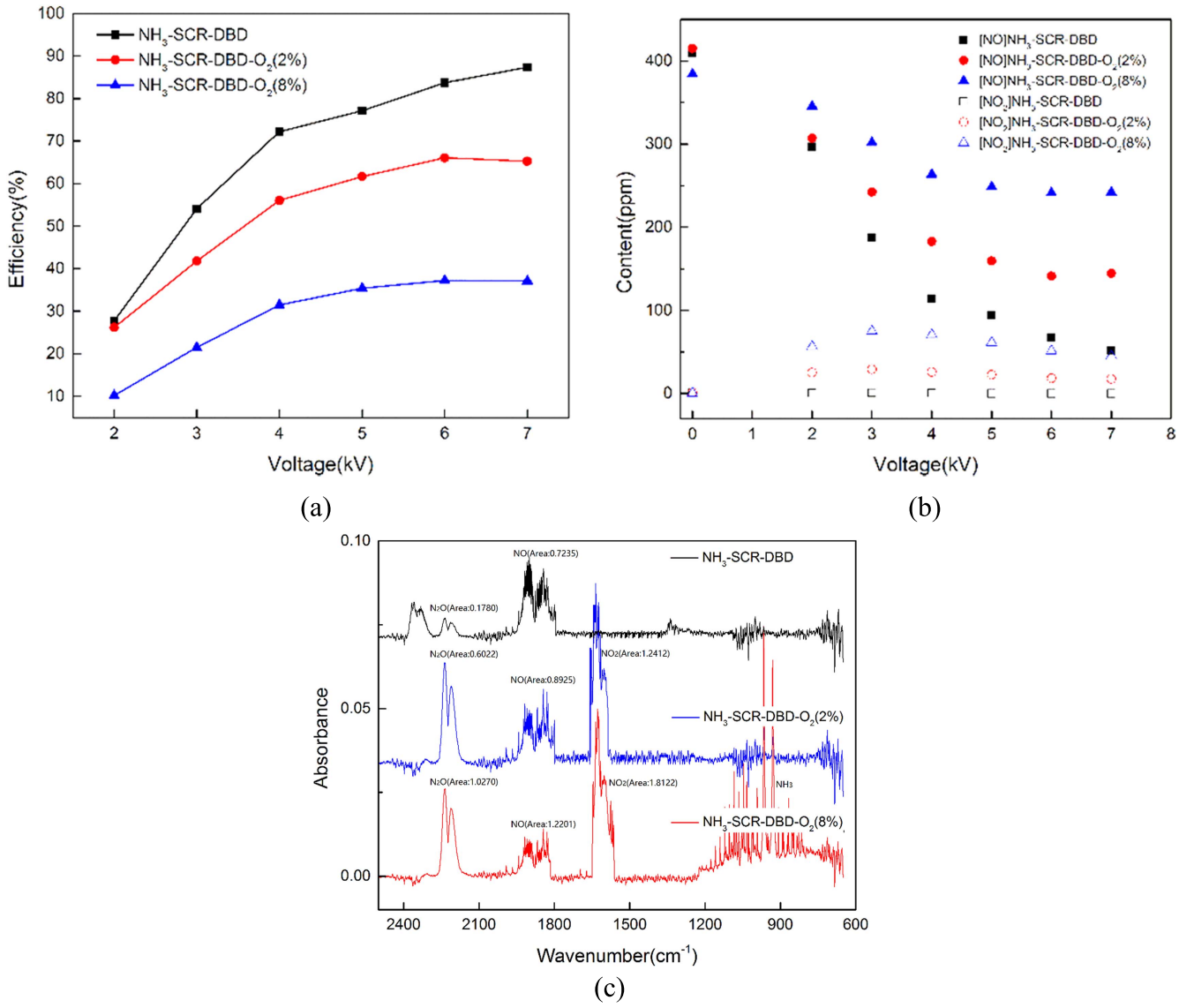

Figure 4. (a) Effects of different oxygen concentration on NO removal efficiency. (b) Effects of different oxygen concentration on NO and NO_2 content. (c) Final products observed using FTIR under different oxygen conditions.

Table 1. Principle reactions involved.

	NO	NO_2
Applied voltage $\leqslant$ 3 kV	$NO + O\cdot \rightarrow O_2 + N_2$ $NO + \cdot OH \rightarrow HNO_2$ $NO + \cdot OH \rightarrow HNO_2$ $4NH_3 + 4NO + O_2 \rightarrow 4N_2 + 6H_2O$ $4NH_3 + 4NO + 3O_2 \rightarrow 4N_2O + 6H_2O$	$NO + \cdot O \rightarrow NO_2$
Applied voltage > 3 kV	$NH + \cdot O \rightarrow H\cdot + NO$ $NH + O_2 \rightarrow \cdot OH + NO$ $NO_2 + \cdot O \rightarrow \cdot OH + NO$	$NH + NO_2 \rightarrow N_2O + \cdot OH$ $NH + NO_2 \rightarrow HO_2\cdot + N_2$ $NH + NO_2 \rightarrow HNO\cdot + NO$

NO molecule production through R6, R7 and R10. The principle reactions are listed in table 1.

Figure 4(c) shows the outlet gas components observed by FTIR under different oxygen conditions at fixed applied voltage of 3 kV. It indicates that the more oxygen was led into the gas stream, the higher the concentrations of N_2O, NO and NO_2 that were observed. The results also indicated that with higher concentration of O_2, NO removal efficiency decreased, but N_2O and NO_2 were increased by the oxidizing reactions of NO and NH_3 molecules in the reactor.

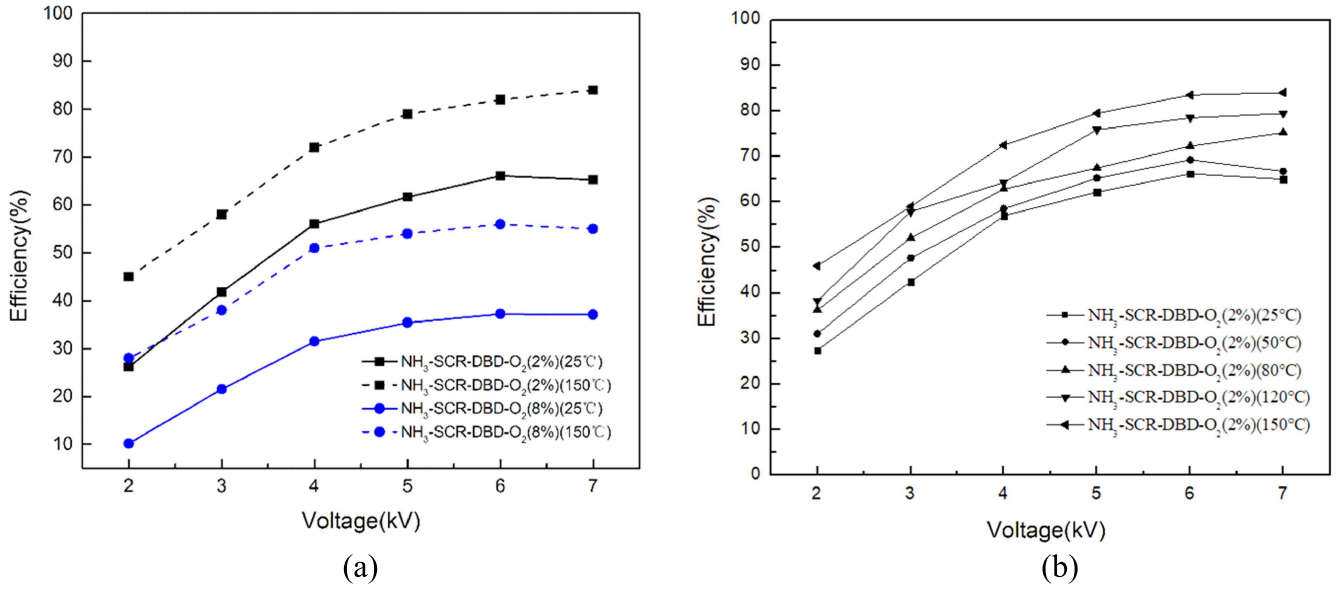

Figure 5. (a) Effects of temperature on NO removal efficiency under different oxygen content. (b) Effects of temperature on NO removal efficiency at 2% oxygen content.

3.3. Temperature effects

Figure 5(a) shows the relationship of NO removal efficiency and applied voltage under different oxygen content (2% and 8%) and temperature (25 °C and 150 °C), and figure 5(b) shows the relationship of NO removal efficiency and applied voltage under different temperatures (25 °C, 50 °C, 80 °C, 120 °C and 150 °C) at 2% oxygen content. The initial concentrations of NO and NH_3 were 400 ppm and 90 ppm, respectively. The applied voltage varied from 2 kV to 7 kV.

The data in figure 5 show that higher temperature conditions were good for the removal efficiency of NO. Under the applied voltage of 7 kV, η_{NO} was improved from 65% to 84% and 37% to 55% in the presence of O_2 of 2% and 8%, respectively. NO removal was influenced by temperature for two main reasons: E/N (electrical field strength divided by the total gas density) and reaction rate [34]. E/N increases when the electric field strength (E) is proportional to the applied voltage if the plasma reactor parameters remain constant and the gas density N decreases with the increase in the temperature [35]. A rising E/N means that more energy is transferred to the particles, which promotes the ionization and excitation process. Then, more active species such as ·O, ·H, ·OH, and NH· are induced into the reactor system and play a role in NO removal. At high temperature conditions, electron detachment becomes significant so that radicals of ·O, ·H, ·OH, and NH· have more negligible effects than their anionic counterparts [36].

Meanwhile, temperature affects the reaction rate coefficients directly, which dominate the chemical kinetic in gas phase reactions. The main reactions involved are shown in table 2.

Among those reactions in table 2, compared to the data at temperatures of 25 °C, the larger rate coefficients of reactions of R1–R2 and R14–R17 at a temperature of 150 °C contribute to the reactions of active radicals with NO. In this system, the removal of NO mainly depends on reactions R17–R22, R3 and R5. More active radicals such as HO_2· and ·O, contribute significantly to the conversion of NO into NO_2 [37]. Moreover, with increasing the temperature, the rate constants of R24 and R25 were decreased, resulting in less NO molecule formation. In general, the generation of active species and the rate coefficients of NO removal reactions were both promoted with increased temperature, and then contributed to η_{NO} considerably. In addition, previous studies [17] showed that at temperatures of about 100 °C, the catalytic activity of the V_2O_5–WO_3/TiO_2 catalyst increases with the increase in temperature; it also promoted the removal of NO.

3.4. Humidity effects

Figure 6 shows the effect of water vapor on NO removal under varied applied voltages of 2–7 kV. The initial concentrations of NO and NH_3 were set at 400 ppm and 90 ppm, respectively. All experiments were conducted at room temperature of 25 °C. The relative humidity in our DBD reactor was 85% in the presence of H_2O.

The results shown in figure 6 indicate that the NO removal efficiency was only 57% in the presence of H_2O, but increased to 72% without H_2O under an applied voltage of 4 kV. In other words, H_2O has an obvious suppression effect on NO removal. The reasons for this phenomenon might be considered as follows.

Firstly, with the addition of H_2O, the electronegative molecules lead to large quantities of electrons absorbed, which decrease the discharge power. In the experiment process we found that the frequency was 14.0 kHz without H_2O and 10.5 kHz after adding H_2O. Previous studies [38] have shown that with H_2O addition, the number of high-energy electrons decreases, which indicates that the collisions

Table 2. Major reactions and their corresponding rate coefficients.

Reactions	Rate coefficients ($cm^3\ s^{-1}$)			Reaction number
	25 °C (298 K)	150 °C (423 K)	Formula	
$e + O_2 \rightarrow e + \cdot O + \cdot O$			$f(E/N)$	R15
$e + H_2O \rightarrow \cdot H + \cdot OH + e$			$f(E/N)$	R16
$e + H_2O \rightarrow H^- + OH$			$f(E/N)$	R17
$e + N_2 \rightarrow e + \cdot N + \cdot N$			$f(E/N)$	R18
$O_2 + \cdot O \rightarrow O_3$	6.0×10^{-34}	9.0×10^{-34}	$6.0 \times 10^{-34}\exp(T/300)^{-2.6}$	R8
$O_2 + H \rightarrow HO_2\cdot$	9.5×10^{-11}	1.1×10^{-10}	$9.47 \times 10^{-11}(T/298)^{0.44}$	R19
$\cdot O + H_2O \rightarrow \cdot OH + \cdot OH$	7.3×10^{-24}	4.1×10^{-20}	$1.84 \times 10^{-}11(T/298)^{0.95}\exp(-71\,255/RT)$	R20
$\cdot OH + NH_3 \rightarrow H_2O + \cdot NH_2$	1.6×10^{-13}	4.0×10^{-13}	$3.5 \times 10^{-12}(T/298)\exp(-7691/RT)$	R1
$NH_3 + \cdot O \rightarrow \cdot OH + \cdot NH_2$	4.4×10^{-17}	7.5×10^{-16}	$2.9 \times 10^{-13}(T/298)^{2.1}\exp(-21\,784/RT)$	R2
NO removal				
$NO + \cdot N \rightarrow N_2 + \cdot O$	2.1×10^{-11}	3.1×10^{-11}	$8.2 \times 10^{-11}\exp(-3409/RT)$	R21
$O_3 + NO \rightarrow O_2 + NO_2$	1.8×10^{-14}	6.3×10^{-14}	$1.4 \times 10^{-12}\exp(-1310/T)$	R22
$HO_2 + NO \rightarrow NO_2 + \cdot OH$	2.7×10^{-13}	1.2×10^{-12}	$3.3 \times 10^{-11}\exp(-11\,890/RT)$	R23
$\cdot O + NO \rightarrow NO_2$	3.0×10^{-11}	3.3×10^{-11}	$3.0 \times 10^{-11}(T/298)^{0.6}$	R24
$\cdot NH + NO \rightarrow N_2O + \cdot H$	2.9×10^{-11}	3.1×10^{-11}	$1.17 \times 10^{-10}(T/298)^{-1.03}\exp(-3492/RT)$	R25
$\cdot OH + NO \rightarrow HNO_2$	7.4×10^{-31}	3.2×10^{-31}	$7.4 \times 10^{-31}(T/300)^{-2.4}$	R26
$NO + NH_2 \rightarrow N_2 + H_2O$	1.2×10^{-11}	9.0×10^{-12}	$2.07 \times 10^{-11}(T/298)^{-1.61}\exp(-1247/RT)$	R3
$\cdot NH + NO \rightarrow \cdot OH + N_2$	4.8×10^{-12}	4.3×10^{-12}	$5.86 \times 10^{-12}(T/298)^{-0.5}\exp(-499/RT)$	R5
NO formation				
$\cdot O + NO_2 \rightarrow NO + O_2$	9.7×10^{-12}	8.6×10^{-12}	$6.51 \times 10^{-12}\exp(998/RT)$	R27
$NH_2 + HNO \rightarrow NH_3 + NO$	3.6×10^{-12}	2.9×10^{-12}	$1.1 \times 10^{-12}(T/298)^{0.41}\exp(2935/RT)$	R28
$O_2 + \cdot NH \rightarrow \cdot OH + NO$	9.0×10^{-15}	1.9×10^{-14}	$6.74 \times 10^{-14}(T/298)^{0.79}\exp(-4997/RT)$	R7
$\cdot O + NH_2 \rightarrow H_2 + NO$	2.1×10^{-13}	2.3×10^{-13}	$7.42 \times 10^{-14}(T/298)^{1.02}\exp(2627/RT)$	R29
$NH_3 + NO_2 \rightarrow HNO_2 + \cdot NH_2$	2.2×10^{-37}	1.5×10^{-31}	$1.11 \times 10^{-15}(T/298)^{3.41}\exp(-12\,4717/RT)$	R30

The rate coefficients were obtained from the NIST chemical kinetics database.

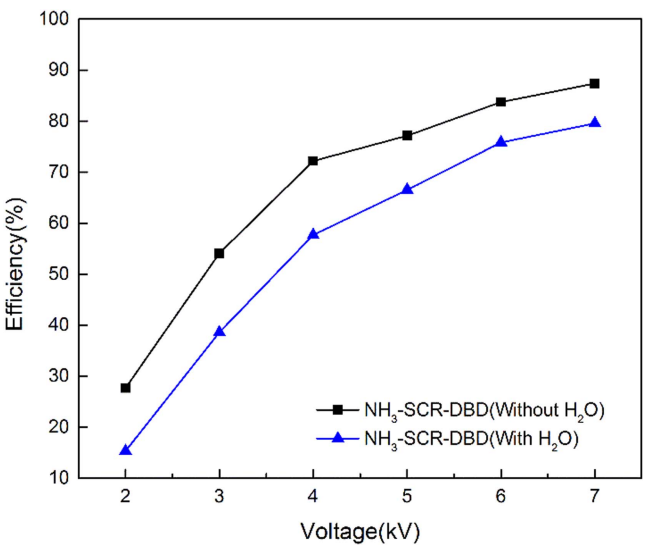

Figure 6. Effects of water on NO removal efficiency.

between electrons and molecules decrease. As fewer electrons are produced, the electric field of the discharge system decreases, and the energy is not high enough to break the bond of neutral molecules such as H_2O and O_2. Furthermore, more H_2O molecules leads to fewer vital active species such as HO·, HO_2· and ·O [39].

Secondly, the formation of active particles induced by the collision between electrons and H_2O molecules such as ·H and ·OH lowers electron abundance. Therefore, the remainder of the electrons do not reach the energy to produce HO_2· and ·O, and the number of active species participating in the NO reduction reaction are reduced, which leads to a decrease in NO removal efficiency.

Thirdly, in the presence of H_2O, more ·OH radicals are produced:

$$H_2O \rightarrow H + \cdot OH \quad \text{(R11)}$$

$$\cdot O + H_2O \rightarrow \cdot OH + \cdot OH. \quad \text{(R16)}$$

The ·OH radicals react with NH_3:

$$\cdot OH + NH_3 \rightarrow H_2O + \cdot NH_2 \quad \text{(R1)}$$

$$\cdot OH + \cdot NH_2 \rightarrow \cdot NH + H_2O \quad \text{(R27)}$$

$$\cdot OH + \cdot NH \rightarrow H_2O + \cdot N \quad \text{(R28)}$$

and the reaction of H_2O with N is intensified by producing more ·HN to contribute to NO formations via the following reactions:

$$H_2O + \cdot N \rightarrow \cdot HN + \cdot OH \quad \text{(R29)}$$

$$HN + \cdot OH \rightarrow NO + H_2 \quad \text{(R30)}$$

$$\cdot OH + NO_2 \rightarrow HO_2\cdot + NO. \quad \text{(R31)}$$

In addition, previous work [40] showed that the presence of H_2O has an inhibiting effect on the catalyst activity, which is caused by competitive adsorption of H_2O and the reactants such as NH_3 and/or NO.

As demonstrated above, water plays a negative effect on NO removal in high relative humidity conditions.

4. Conclusions

Our study mainly investigated NO removal using a new integrated NH_3–SCR–DBD reactor with ammonia (NH_3) as a reductant. Catalysts (V_2O_5–WO_3/TiO_2) were inserted in the discharge area. In this paper, the effects of NH_3, O_2, temperature and H_2O on NO removal were discussed. Results showed that the NO removal efficiency increases with the increase in NH_3 and temperature, but decreased with the increase in O_2 and H_2O. Meanwhile, when the gas concentration ratio of NH_3/NO was 0.23–0.67, we obtained acceptable NO removal efficiency with low energy consumption. When the temperature increased to 150 °C, more active species such as ·O, ·H, ·OH and NH· were produced, which promoted NO removal. In the presence of H_2O, the discharge state was suppressed and ·OH generated from the dissociation of H_2O led to new NO formation. The combination of NH_3–SCR assisted by the DBD reactor method was demonstrated to be a very attractive and promising method for NO removal application.

Acknowledgments

The financial support for this research was provided by National Natural Science Foundation of China (No. 21577023), the Key Project supported by the Science and Technology Commission of Shanghai Municipality (No. 15DZ1205904), and Technology Innovation and Energy Saving Enhancement Project supported by Shanghai SASAC (No. 2013019). The authors thank Xu Cao, Jianyuan Hou for their help in the research work.

ORCID iDs

Yanghaichao LIU (刘杨海超) https://orcid.org/0000-0001-6557-6818

References

[1] Liu Y X, Wang Q and Pan J F 2016 *Environ. Sci. Technol.* **50** 12966
[2] Huang T J, Wu C Y and Lin Y H 2011 *Environ. Sci. Technol.* **45** 5683
[3] Xiong S C *et al* 2015 *Ind. Eng. Chem. Res.* **54** 11011
[4] Georgiadou I *et al* 1998 *J. Phys. Chem.* B **102** 8459
[5] Qiu Y *et al* 2016 *Chem. Eng. J.* **294** 264
[6] Guan B *et al* 2011 *Ind. Eng. Chem. Re.* **50** 5401
[7] Dahlin S *et al* 2016 *Appl. Catal. B* **183** 377
[8] Shen B X *et al* 2016 *Ind. Eng. Chem.* **25** 262
[9] Gao G *et al* 2017 *Appl. Surf. Sci.* **411** 338
[10] Gao F *et al* 2017 *Chem. Eng. J.* **317** 20
[11] Sun P *et al* 2017 *Appl. Catal. A* **531** 129
[12] Xu H M *et al* 2016 *Appl. Catal. B* **186** 30
[13] Vuong T H *et al* 2016 *Appl. Catal. B* **197** 159
[14] Phil H H *et al* 2008 *Appl. Catal. B* **78** 301
[15] Jangjou Y *et al* 2016 *ACS Catal.* **6** 6612
[16] Zhang L *et al* 2016 *Chem. Eng. J.* **296** 122
[17] Magnusson M, Fridell E and Ingelsten H H 2012 *Appl. Catal. B* **s111–122** 20
[18] Benrabbah R *et al* 2017 *Catal. Commun.* **89** 73
[19] Nizio M *et al* 2016 *Catal. Commun.* **83** 14
[20] Jwa E *et al* 2013 *Fuel Process. Technol.* **108** 89
[21] Pan H and Qiang Y 2014 *Plasma Chem. Plasma Process.* **34** 811
[22] Patil B S *et al* 2016 *Appl. Catal. B* **194** 123
[23] Niu J H *et al* 2008 *Plasma Sci. Technol.* **10** 466
[24] Kogelschatz U 2003 *Plasma Chem. Plasma Process.* **23** 1
[25] Broer S and Hammer T 2000 *Appl. Catal. B* **28** 101
[26] Wang T *et al* 2017 *Fuel Process. Technol.* **158** 199
[27] Li F L *et al* 2013 *Plasma Sources Sci. Technol.* **22** 065003
[28] Li Z, Zhao Z and Li X H 2013 *Phys. Plasmas* **20** 013503
[29] Atkinson R *et al* 2004 *Atmos. Chem. Phys.* **4** 1461
[30] Cohen N and Westberg K R 1991 *J. Phys. Chem. Ref. Data* **20** 1211
[31] Hack W, Schacke H, Schröter M and Wagner H Gg 1979 *Symp. Int. Combust. Proc.* **17** 505
[32] Bozzelli J W, Chang A Y and Dean A M 1994 *Symp. Int. Combust. Proc.* **25** 965
[33] Römming H J and Wagner H G 1996 *Symp. Int. Combust. Proc.* **26** 559
[34] Chang M B and Yang S C 2001 *AIChE J.* **47** 1226
[35] Li S, Tang Z C and Gu F 2010 *Heat Mass Transfer* **47** 851
[36] Tanthapanichakoon W *et al* 2004 *Chem. Eng. J.* **97** 213
[37] Zhu A M *et al* 2005 *Plasma Chem. Plasma P.* **25** 371
[38] Wang T *et al* 2013 *Plasma Chem. Plasma P.* **33** 681
[39] Messaoudi R *et al* 1996 *IEEE Trans. Dielectr. Electr. Insul.* **3** 537
[40] Huang Z G, Zhu Z P and Liu Z Y 2002 *Appl. Catal. B* **39** 361